NUCLEAR THEORY, Vol. 31 (2012)
eds. A. Georgieva, N. Minkov, Heron Press, Sofia

Systematics of Nuclear Surface Vibrations in Deformed Nuclei

G. Popa
Ohio University Zanesville, 43701 OH, USA

Abstract. The low-energy spectra and electromagnetic transitions for a series of heavy deformed nuclei are analyzed in the framework of the pseudo-SU(3) model. A realistic Hamiltonian with proton and neutron single particle energies, monopole pairing interaction, in addition to the quadrupole-quadrupole term, is used. The strengths of the interactions are fixed with values from systematics. The effect of the single-particle energies on the overall spectra and electromagnetic transition is analyzed.

1 Introduction

The pseudo-SU(3) model has been proven to be a good tool for calculating the electromagnetic transitions in heavy deformed nuclei [1]. The model has been applied successfully to a series of even-even [2–4, 8] and odd-mass [5–7] heavy deformed nuclei. The first step in any application of the pseudo-SU(3) model is to build a many-body basis. For the pseudo-SU(3) scheme the proton and neutron valence Nilsson single-particle levels are filled from below for a fixed deformation, which in the case of ^{160}Dy is $\epsilon_2 = 0.25$ [9]. It allows the determination of the most probable normal and unique parity orbital occupancies. Of the 16 valence protons, 8 occupy normal parity orbitals, and 8 intruder orbitals. Of the 12 valence neutrons, 8 are in normal parity orbitals and 4 in intruder orbitals. Since for some nuclei, this particle distribution on normal and intruder orbitals becomes difficult, the orbitals beeying very close together, the effect of the strength of the single particle energies on the low-energy spectra and electromagnetic transitions was analyzed. We studied this effect in $^{160-162}$Dy and ^{168}Er nuclei.

Results for energy levels of the four lowest-lying bands in ^{160,162}Dy and ^{168}Er, as well as $B(E2)$ transition strengths between the levels and the $B(M1)$ strength distribution of the ground-state are reported. Calculations were carried out within the framework of pseudo-SU(3) model using realistic single-particle energies and quadrupole-quadrupole and pairing interaction strengths fixed from systematics, while four "rotor like" terms were adjusted nucleus-by-nucleus to obtain the best description of each energy spectrum. Comparison with experimental energies and $B(E2)$ transition strengths is in general very favorable. However, some excited bands are predicted to be too high in energy. Including other terms in the Hamiltonian would probably correct this effect. Scaling

down the single-particle energies allows a nearly perfect description of the energy spectra. In the same time, electromagnetic transitions are calculated in the three nuclei, with regular and reduced single particle strength.

2 Model Interaction

The Hamiltonian consists of quadrupole-quadrupole ($Q \cdot Q$), proton (π) and neutron (ν) single particle energies ($H^{\pi}_{sp} + H^{\nu}_{sp}$), proton and neutron pairing (H^{π}_{P} and H^{ν}_{P}), as well as the rotor part (H_{ROT}).

$$H = \chi Q \cdot Q + H^{\pi}_{sp} + H^{\nu}_{sp} - G_{\pi} H^{\pi}_{P} - G_{\nu} H^{\nu}_{P} + H_{ROT} \tag{1}$$

where

$$H_{ROT} = aJ^2 + bK^2_J + a_3 C_3 + a_{sym} C_2 \tag{2}$$

C_2 and C_3 terms are the second and third order Casimir invariants of SU(3), which are related to the deformation of the nucleus. J^2 is the total angular momentum operator. K^2_J is the K-band splitting operator resolving the multiple occurrences of the same angular momentum within an SU(3) irreducible representation (irrep). The single particle energies are calculated in the standard way:

$$H^{\sigma}_{sp} = H_0 + c\hat{l}\hat{s} + d\hat{l^2} = H_{OSC} - \hbar\bar{\omega}_0 \kappa (2\hat{l}.\hat{s} + \mu\hat{l^2}) \tag{3}$$

where $\sigma = \pi$ or ν, H_0 is the spherical oscillator for which SU(3) is an exact symmetry, and the constants values are taken from [10]. For ^{160}Dy the $\hbar\omega_0 = 41$ MeV $\times A^{-1/3} = 7.55$ MeV is the oscillator constant for the equivalent spherical nucleus and the constants κ and μ have the values [10]: $\kappa_{\pi} = 0.06370$, $\kappa_{\nu} = 0.60$, $\mu_{\pi} = 0.06370$, and $\mu_{\nu} = 0.42$.

3 Parameters

Pseudo-SU(3) model was used to calculate the normal parity bands in the ^{160}Dy, ^{162}Dy, and ^{168}Er nuclei. These nuclei exhibit rotational ground-state bands and a few $K^{\pi} = 0^{+}$ band heads below 2 MeV. As in other applications of the pseudo-SU(3) model [2, 3, 5], approximatively twenty pseudo-SU(3) irreps with the largest values of the second order Casimir operator C_2 ($Q \cdot Q = 4C_2 - 3L^2$) are used in building the basis states. For example, for ^{162}Dy the first twenty-one irreps with the largest C_2 values were used. Strengths of the quadrupole-quadrupole and pairing interactions were fixed, respectively, at values typical of those used by other authors: $\chi = 35\ A^{5/3}\ MeV$; $G_{\pi} = 21/A\ MeV$ and $G_{\nu} = 19/A\ MeV$. Calculations were carried out with the single-particle orbit-orbit (l^2) interaction strengths fixed by systematics [10],

$$D_{\sigma}(\sigma = \pi, \nu) = \hbar\omega\kappa_{\sigma}\mu_{\sigma}, \tag{4}$$

where $\hbar\omega = 41/A^{1/3}$, and κ_σ and μ_σ are assigned their usual harmonic oscillator values [10]:

$$\begin{aligned} \kappa_\pi &= 0.0637, \ \mu_\pi = 0.60 \\ \kappa_\nu &= 0.0637, \ \mu_\nu = 0.42. \end{aligned} \tag{5}$$

Hence, the a_3 parameter was varied to yield a best fit to the energy of the second 0^+ state; the energy of the third 0^+ was not included in the fitting procedure and as the results given below show, falls higher than the experimental number for all of the nuclei considered.

As we have learned from the previous calculations [3, 4, 8], the other three parameters do not change the band-head energy of the second excited $K^\pi = 0^+$ band, but they can adjust the other bands. Therefore, the a_{sym} parameter was adjusted to give a best fit to the first 1^+ state, b was fitted to the value of the band-head energy of the $K^\pi = 2^+$ band, and a was varied to get the moment of inertia of the ground-state band correct. The full set of parameters is given in Table 1. All of these four fitted parameters vary smoothly from one nucleus to another. Actually, all four "free" parameters decrease as the mass number "A" increases. The J^2 interaction strength decreases from 1.0×10^{-3} for ^{160}Dy to -2.1×10^{-3} for ^{168}Er, and the interaction strength of K_J^2 operator decreases from 0.10 for ^{160}Dy to 0.022 for ^{168}Er. The a_{sym} parameter that is fitted to the energy of the first 1^+ state also decreases from 1.45×10^{-3} for ^{160}Dy to 0.80×10^{-3} for ^{168}Er. The nucleus ^{168}Er has one more pair of protons than the Dysprosium nuclei. Since "A" is larger for ^{168}Er than for the Dy isotopes, one might expect even smaller values for the parameters, and while this is what is observed for a and a_{sym}, the extra proton pair requires values for b and a_3 that are smaller than the ones for ^{160,162}Dy.

Since some excited bands are predicted to be too high in energy, we may miss some of the states in the energy gap. Other interactions, not yet included

Table 1. Parameters used for ^{160,162}Dy and ^{168}Er nuclei, in the pseudo-SU(3) Hamiltonian (1).

Parameter	^{168}Er	^{162}Dy	^{160}Dy
$\hbar\omega$	7.40	7.52	7.55
$\chi \times 10^{-3}$	6.84	7.27	7.42
D_π	-0.283	-0.287	-0.289
D_ν	-0.198	-0.201	-0.202
G_π	0.125	0.130	0.131
G_ν	0.101	0.105	0.106
a $\times 10^{-3}$	-2.1	0.0	1.0
b	0.022	0.08	0.10
$a_{sym} \times 10^{-3}$	0.80	1.40	1.45
$a_3 \times 10^{-4}$	0.75	1.32	1.36

Table 2. The second set of parameters used in the pseudo-SU(3) Hamiltonian corresponding to reduced one-body interaction strengths.

Parameter	^{168}Er	^{162}Dy	^{160}Dy
$\chi \times 10^{-3}$	6.84	7.27	7.42
D_π	-0.153	-0.187	-0.141
D_ν	-0.107	-0.131	-0.099
G_π	0.125	0.130	0.131
G_ν	0.101	0.105	0.106
a $\times 10^{-3}$	-2.1	-1.6	-1.0
b	0.072	0.11	0.14
$a_{sym} \times 10^{-3}$	0.80	0.80	0.67
$a_3 \times 10^{-4}$	0.18	0.80	0.64

in the Hamiltonian, may be responsible. Instead of introducing other terms, however, we show that scaling down the single-particle energies allows a nearly perfect description of the energy spectra. In this case, the a_3 parameter was again allowed to vary to gain the best fit to the energies of both the second and third 0^+ states. Allowing for a scaling of the D_σ ($\sigma = \pi, \nu$) parameters, meant that a, b, a_{sym}, and a_3 had to be readjusted. The new parameter set is given in Table 2.

4 Energy Spectra

The experimental and calculated energies of the lowest four energy bands in ^{162}Dy are compared in Figure 1. For illustrative purposes, the energies and $M1$ transition spectra are shown together for the two parameter sets used in the calculations, from Tables 1 and 2. For both sets, the calculated results are in good agreement with experiment. Likewise, the $B(E2)$ transition probabilities are in excellent agreement with the experimental data. As an example, the values for ^{162}Dy are given in Table 4.

The energy spectra calculated by diagonalizing the Hamiltonian (1), with parameters from Table 1, are in excellent agreement with the experimental data for the first three low-energy bands. These spectra are given in the left-hand-side plot of the Figure1. The differences between the calculated and experimental energy values are less than 5% for the ground-state bands for all nuclei, less than 5% in the first exited $K = 0^+$ band of ^{160}Dy, ^{162}Dy, and ^{168}Er, less than 5% in the $K = 2^+$ band of ^{164}Dy, and less than 10% in the $K = 2^+$ of ^{160}Dy, ^{162}Dy, and ^{168}Er. The states in the second excited $K = 0^+$ bands are higher in values by about $0.5\ MeV$ than the experimental ones. The moment of inertia for this band is higher than the experimental one.

When D_σ ($\sigma = \pi,\ \nu$) were scaled down to fit both excited 0^+ energies, few other improvements were obtained. The whole $K = 0_3^+$ band moved down in energy and the levels inside it were compressed such that the difference between these calculated energies and the experimental ones ended up being less than

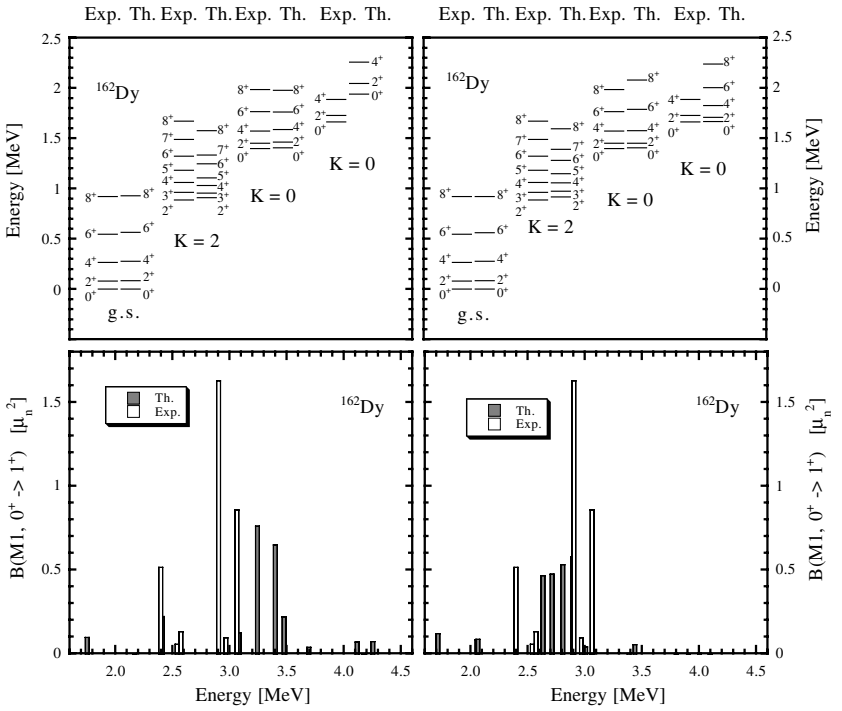

Figure 1. Energy spectra of ^{162}Dy obtained using Hamiltonian given by eq. (1) with parameters from Table 1 (left side) and from Table 2 (right side). 'Exp.' represents the experimental results and 'Th.' the calculated ones. The lower plot gives the theoretical and experimental $M1$ transition strengths from the $J^\pi = 0^+$ ground-state to the various $J^\pi = 1^+$ levels.

7%. The description of the $K = 2^+$ band also improved. There was very little change in the ground-state band, and also the $K = 0_2^+$ band changed very little. Similar results were obtained for ^{160}Dy and ^{168}Er. The difference in energy between the calculated and experimental band-heads of the second excited $K=0$ bands increases as the mass number A increases. For ^{160}Dy and ^{162}Dy the difference is about $0.3MeV$ while for ^{168}Er is about $0.65MeV$. The states in the second excited $K = 0$ band are well defined. The results suggest that it may be interesting to see how the parameters change with changing the proton rather than the neutron number.

4.1 $B(E2)$ Strengths and Wave Functions

Very good agreement with experimental $B(E2)$ strengths was achieved for transitions in the ground-state band in both calculations. As an example, the intra-

Table 3. SU(3) content of calculated four band-head states in ^{162}Dy. The percentage distributions of each state across the (λ, μ) values are given in the second and third columns for calculations in the two cases. All the basis states that contribute to more than 2% are identified.

$J_{\#}$	th1.	th2.	(λ_π, μ_π)	(λ_ν, μ_ν)	(λ, μ)
0_1	59.3	64.0	(10, 4)	(18, 4)	(28, 8)
	6.5	7.4	(10, 4)	(18, 4)	(30, 4)
	20.1	7.3	(10, 4)	(20, 0)	(30, 4)
	7.1	5.1	(12, 0)	(18, 4)	(30, 4)
	2.7	3.1	(10, 4)	(18, 4)	(32, 0)
	3.0	-	(12, 0)	(20, 0)	(32, 0)
2_γ	81.4	85.9	(10, 4)	(18, 4)	(28, 8)
	5.2	4.9	(10, 4)	(20, 0)	(30, 4)
	4.6	3.0	(12, 0)	(18, 4)	(30, 4)
	4.5	2.6	(4, 10)	(18, 4)	(22, 14)
0_a	91.8	63.4	(4, 10)	(18, 4)	(22, 14)
	4.2	-	(10, 4)	(20, 0)	(30, 4)
	-	10.3	(10, 4)	(18, 4)	(28, 8)
	-	20.2	(10, 4)	(20, 0)	(30, 4)
	-	5.0	(12, 0)	(18, 4)	(30, 4)
0_b	33.3	17.6	(10, 4)	(18, 4)	(28, 8)
	47.0	40.2	(10, 4)	(20, 0)	(30, 4)
	11.0	9.7	(12, 0)	(20, 0)	(32, 0)
	5.9	27.0	(4, 10)	(18, 4)	(22, 14)
	-	3.1	(12, 0)	(18, 4)	(30, 4)

band $B(E2)$ transition strengths are given for ^{162}Dy in Table 4. The intra-band transition strengths for the other three bands, calculated in the two situations with interaction strengths from Tables 1 and 2, are also given. Inter-band transition probabilities are given for a few cases where experimental numbers exist (Table 6). In the present calculations, unlike in the ^{158}Gd [8], the inter-band $B(E2)$ strengths are overestimated in both cases. It looks like the strength of the single-particle energies does not affect the strength of the B(E2) transitions. We will calculate these transitions for more nuclei to have a clear conclusion.

Note that the strengths of the $B(E2)$ transition probabilities are consistent across all four bands (Tables 4 and 5). In all tables the theoretical $B(E2)$ transition probabilities are given for the two sets of calculations corresponding to the parameters from Tables 1 and 2. The differences in these values are very small, at the third digit in the ground-state and $K^\pi = 2^+$ bands, and at the second digit in the other two bands.

When reduced one-body interaction strengths are used, the calculated low-lying energy spectra are found to be in excellent agreement with experimental

Table 4. Theoretical and experimental intra-band $B(E2)$ transition strengths in ^{162}Dy in the $K^\pi = 0_1^+$ band, calculated in the two situations. The third and fourth columns refer to calculations done using parameters from table 1 and 2, respectively.

	$B(E2; J_i \to J_f)$ (e^2b^2)		
$J_i \to J_f$	Exp.	Theory 1	Theory 2
$0_1 \to 2_1$	5.134 ± 0.155	5.134	5.133
$2_1 \to 4_1$	2.675 ± 0.102	2.635	2.634
$4_1 \to 6_1$	2.236 ± 0.127	2.325	2.321
$6_1 \to 8_1$	2.341 ± 0.115	2.201	2.193

data for all four bands of the four nuclei considered. Eigenstates are calculated for angular momenta up to $8\hbar$. This leads to a prediction of some new levels in the $K^\pi = 2^+$ band as well as in the first and second excited $K^\pi = 0^+$ bands. In all cases these levels have strong intra-band $B(E2)$ transition probabilities.

As in previous works [3,4,8], although the basis is strongly truncated, being built from about twenty SU(3) irreps, not all of these play an important role. All the basis states that contribute to more than 2% are identified and presented in Table 3 in ^{162}Dy. In the same time, the SU(3) content stays almost the same for all the states in a band. The SU(3) content of the wave functions calculated for Dysprosium nuclei shows also that only few irreps are important. Furthermore these irreps are the same in all the states within one band, and their percentages vary slowly from the low angular momentum states towards the higher angular momentum states. Details about the SU(3) content of the wave functions as a function of angular momentum, will be published somewhere else.

The components of each state belonging to the ground-state band are about 60% $[(10,4)_\pi \times (18,4)_\nu](28,8)$, that is the leading irrep; 20% $[(10,4)_\pi \times (20,0)_\nu](30,4)$; 7% $[(12,0)_\pi \times (18,4)_\nu](30,4)$; and less from $[(10,4)_\pi \times (18,4)_\nu]$ coupled to $(30,4)$, $[(10,4)_\pi \times (18,4)_\nu](32,0)$, $[(12,0)_\pi \times (20,0)_\nu](32,0)$ and $[(10,4)_\pi \times (16,5)_\nu](26,9)$. These (30,4) and (32,0) representations contribute less and less as the angular momentum increases within the band, and the last one occurs only for angular momenta 6 and 8, and contributes less than 4%. In the $K^\pi = 2^+$ band, the representations that contribute the most to the wave functions are the same as in the ground-state band.

In the first excited $K = 0^+$ band the dominant SU(3) irrep is (22,14), but unlike for the Gadolinium nuclei, here the (22,14) irrep is the dominant irrep, namely, 92% $[(4,10)_\pi \times (18,4)_\nu]$ and 4% $[(10,4)_\pi \times (20,0)_\nu](30,4)$.

In the second excited 0^+ band the dominant irrep is $[(10,4)_\pi \times (20,0)_\nu](30,4)$, with 47% in the 0^+ state, and its strength is decreasing to only 4% in the 8^+ state. In the 0^+ state there are other three configurations with relatively strong percentages, 34% $[(10,4)_\pi \times (18,4)_\nu](28,8)$, 11% $[(12,0)_\pi \times (20,0)_\nu](32,0)$ and 6% $[(4,10)_\pi \times (18,4)_\nu](22,14)$, which are decreasing in strength as one moves up to the 8^+ state.

Table 5. Calculated intra-band $B(E2)$ transition strengths in ^{162}Dy, in the $K = 2$, $K = 0_2$, and $K = 0_3$ bands, calculated in the two situations. The third and fourth columns refer to calculations done using parameters from Table 1 and 2, respectively. The energies are labeled with the subindex γ for the $K = 2$ band, a, and b for the first and second excited $K = 0$ bands.

		$B(E2; J_i \to J_f)$ (e^2b^2)	
Band	$J_i \to J_f$	Theory 1	Theory 2
$K = 2$	$2_\gamma \to 3_\gamma$	2.480	2.513
	$2_\gamma \to 4_\gamma$	1.060	1.066
	$3_\gamma \to 4_\gamma$	1.630	1.655
	$4_\gamma \to 5_\gamma$	1.145	1.160
	$4_\gamma \to 6_\gamma$	1.625	1.632
	$5_\gamma \to 6_\gamma$	0.716	0.716
	$6_\gamma \to 7_\gamma$	0.607	0.615
	$6_\gamma \to 8_\gamma$	1.685	1.698
$K = 0_2$	$0_a \to 2_a$	4.193	4.581
	$2_a \to 4_a$	2.272	2.435
	$4_a \to 6_a$	2.153	2.173
	$6_a \to 8_a$	2.175	2.030
$K = 0_3$	$0_b \to 2_b$	3.517	3.780
	$2_6 \to 4_b$	1.901	2.184
	$4_b \to 6_b$	2.017	2.076
	$6_b \to 8_b$	2.030	2.052

When the unscaled one-body interaction strengths are used, levels of the first three energy bands are in good agreement with the experimental data. The fourth band is approximately $0.5\ MeV$ higher in energy than observed. The percentage distribution of these eigenstates across the (λ, μ) values changes very little for the first three bands as the one-body interaction strength is scaled. These distributions are given in the second and third columns of Table (3), corresponding to the first and second set of parameters, for the band-head energies of the four

Table 6. Theoretical and experimental, inter-band $B(E2)$ transition strengths in ^{162}Dy, in the two situations. The third and fourth columns refer to calculations done using parameters from Table 1 and 2, respectively. The energies are labelled with the subindex g for the ground-state and γ for the $K^\pi = 2^+$ bands.

	$B(E2; J_i \to J_f)$ (e^2b^2)		
$J_i \to J_f$	Exp.	Theory 1	Theory 2
$2_\gamma \to 4_g$	0.000017 $\pm$ 0.000001	0.006489	0.007311
$0_g \to 2_\gamma$	0.000632 $\pm$ 0.000042	0.2236	0.219120
$2_g \to 2_\gamma$	0.000210	0.0758	0.08209

bands considered. As the second excited $K^\pi = 0^+$ band goes up in energy, the wavefunction content changes slightly and the first and second excited $K^\pi = 0^+$ bands switch order. Likewise, the $M1$ distribution looks $\sim 0.5MeV$ higher in value.

The first excited 1^+ state (calculated using the first set of parameters) lies very close to the experimental one. Moreover this being the band-head of the $K^\pi = 1^+$ band, the band is also well described.

4.2 $M1$ Transition Strengths

The basic structure of the strength distribution is determined by the SU(3)-preserving symmetry part of the Hamiltonian,

$$H_{\mathrm{SU(3)}} = -1/2\chi Q \cdot Q + a_{sym}C2 + aJ^2 + bK_J^2, \tag{6}$$

which embodies strong selection rules [11], namely, there is no coupling between different SU(3) irreps. In this case there are at most four $M1$ transitions between the 0^+ ground-state and 1^+ states. In this case, the calculated $M1$ strengths are concentrated in only two to four states, instead of beying fragmented as observed experimentally. By including SU(3)-symmetry breaking terms in the Hamiltonian, namely, the one-body proton and neutron angular momentum $l^2_{i_{\pi,\nu}}$ and the two-body pairing terms $H_P^{\pi,\nu}$, this theory includes a breakup of the $M1$ strength into relatively closely packed levels centered around the sharp peaks of the pure-SU(3) limit of the theory. As a consequence of the symmetry breaking we find a number of transitions close to the experimentally observed ones. However, some of them have very small transition strengths.

The $M1$ transition strengths derived from the eigenvectors are given along with the experimental results in the lower part of the Figure1. The centroids of the experimental and theoretical $M1$ distributions lie at about the same energy for calculations done with scaled single-particle strengths. By using the parameters from Table 2, the first 1^+ energies are very close to the experimental values, and the calculated and experimental $M1$ distributions span the same energy range. The fragmentation of the $M1$ strength that is predicted (and observed) is a result of symmetry breaking, which is generated by the single-particle and pairing interactions, that are an integral part of the Hamiltonian given by eq. (1). More details for all three nuclei will be published somewhere else.

The total $M1$ strength, which for the full Hamiltonian is lower than for its pure SU(3) limit due to interference generated by the mixing, also shows reasonable reproduction of the experimental data, in most cases slightly underestimated. The calculated total $M1$ strength is very close to the experimental one for ^{160}Dy and ^{162}Dy in both situations, with parameters from Table 1 and Table 2. In the pure SU(3) limit it is almost 50% larger.

Overall, good agreement with experimental data was obtained for describing the $M1$ distributions. The strong transitions occur in the same energy range as the predicted 1^+ states, the transitions are fragmented and clustered around

strong peaks, and the total $M1$ strengths for this energy range agree within the limitations of the model space.

In conclusion, very good description of the first 4 bands in the low-energy spectra and electromagnetic transitions, B(E2) and B(M1) were obtained, in a small truncated basis. The coefficients in the Hamiltonian vary smoothly from one nucleus to another. The single-particle energies strengths do not seem to affect the strength of the electromagnetic transition, but do affect the low-energy spectrum. The model and procedure will be applied to more nuclei in the region, to obtain a consistent procedure for fixing the interaction strengths.

References

[1] J.P. Draayer, K.J. Weeks, and K.T. Hecht, *Nucl. Phys. A* **381** (1982) 1; J.P. Draayer and K.J. Weeks, *Ann. of Phys.* **156** (1984) 41; O. Castaños, J.P. Draayer, and Y. Leschber, *Ann. of Phys.* **180** (1987) 290; O. Castaños, J.P. Draayer, and Y. Leschber, *Z. Phys.* **329** (1988) 33.

[2] T. Beuschel, J.G. Hirsch, and J.P. Draayer, *Phys. Rev. C* **61** (2000) 54307.

[3] G. Popa, J.G. Hirsch and J.P. Draayer, *Phys. Rev. C* **62** (2000) 064313.

[4] G. Popa, A. Georgieva and J.P. Draayer, *Phys. Rev. C* **69** (2004) 064307.

[5] C.E. Vargas, J.G. Hirsch, T. Beuschel, and J.P. Draayer, *Phys. Rev. C* **61** 31301 (2000).

[6] C.E. Vargas, J.G. Hirsch, and J.P. Draayer, *Nucl. Phys. A* **673** (2000) 219. 22.

[7] C.E. Vargas, J.G. Hirsch, and J.P. Draayer, *Phys. Rev. C* **64** (2001) 034306.

[8] J.G. Hirsch, G. Popa, S.R. Lesher, A. Aprahamian, C.E. Vargas, J.P. Draayer, *Rev. Mex. Fis.* **52** (2006) 69-74.

[9] P. Möller, J.R. Nix, W.D. Myers, and W.J. Swiatecki, *At. Data Nucl. Data Tables* **59** (1995) 185.

[10] P. Ring and P. Schuck, *The Nuclear Many-Body Problem* (Springer, Berlin, 1979).

[11] O. Castaños, J.P. Draayer, and Y. Leschber, *Ann. Phys*. **180** (1987) 290.